

The University of Akron

IdeaExchange@UAkron

Williams Honors College, Honors Research
Projects

The Dr. Gary B. and Pamela S. Williams Honors
College

Spring 2020

Comparision of Fillet-Welded Base Plate Fatigue Design for Highway Support Structures with Laboratory Research Tests

William Shea
wrs20@ziips.uakron.edu

Follow this and additional works at: https://ideaexchange.uakron.edu/honors_research_projects



Part of the [Civil Engineering Commons](#), [Manufacturing Commons](#), and the [Structural Engineering Commons](#)

Please take a moment to share how this work helps you [through this survey](#). Your feedback will be important as we plan further development of our repository.

Recommended Citation

Shea, William, "Comparision of Fillet-Welded Base Plate Fatigue Design for Highway Support Structures with Laboratory Research Tests" (2020). *Williams Honors College, Honors Research Projects*. 1158.

https://ideaexchange.uakron.edu/honors_research_projects/1158

This Dissertation/Thesis is brought to you for free and open access by The Dr. Gary B. and Pamela S. Williams Honors College at IdeaExchange@UAkron, the institutional repository of The University of Akron in Akron, Ohio, USA. It has been accepted for inclusion in Williams Honors College, Honors Research Projects by an authorized administrator of IdeaExchange@UAkron. For more information, please contact mjon@uakron.edu, uapress@uakron.edu.

**Comparison of Fillet-Welded Base Plate Fatigue Design for Highway Support Structures
with Laboratory Research Tests**

Submitted To: The University of Akron Williams Honors College

Submitted By: William Shea
Department of Civil Engineering
The University of Akron
Akron, OH 44325
Email: wrs20@uakron.edu

Project Sponsor: Dr. Craig Menzemer

Submission Date: April 24, 2020

ABSTRACT

There are many types of vertical structures along highways that serve unique purposes. These structures include traffic signs for directing, warning, or regulating traffic, luminaires for distributing and directing light, traffic signals supporting equipment such as traffic lights, and combination structures including any combination of the aforementioned structures. Highway support structures are typically fabricated from steel or aluminum and are designed to the guidelines and specifications of the *AASHTO Standard Specifications for Structural Supports for Highway Signs, Luminaires, and Traffic Signals*. The structures are connected to a foundation by anchor bolts through a welded base plate. Often a cause for concern of these welded base plates is that welded structures subjected to repeated loads can display crack growth or fatigue. This report will focus on comparing the *Standard Specifications for Structural Supports for Highway Signs, Luminaires, and Traffic Signals* base plate fatigue design with research of fatigue testing in common base plate details.

TABLE OF CONTENTS

1. Introduction.....	4
1.1. Highway Support Structures	4
1.2. Fatigue and Fatigue Resistance.....	5
2. Fatigue Design and Research.....	7
2.1. AASHTO Standard Specifications for Structural Supports.....	7
2.2. Unstiffened Socket Connection	8
2.3. Stiffened Socket Connection.....	11
3. Finite Element Analysis.....	13
3.1. Finite Element Model	13
4. Summary	17
5. Appendix A.....	18
6. References.....	22

LIST OF FIGURES AND TABLES

Figure 1.1.1. Shoe base plate (a), and stiffened (b) and unstiffened (c) tube-to-transverse base plate.....	5
Figure 1.2.1. Stress Range vs. Number of Cycles (AASHTO LRFD, 2015).	6
Figure 2.2.1. Unstiffened fatigue coefficients and design life (Choi and Najm, 2020).....	10
Figure 2.2.2. Fatigue test results for specimen Type I (Roy et al., 2011).....	11
Figure 2.3.1. Stiffened fatigue coefficients and design life. (Choi and Najm, 2020).	12
Figure 2.3.2. Fatigue test results for specimen Type XII at stiffener top (Roy et al., 2011).	13
Figure 3.1.1. ANSYS stiffened socket connection (Choi and Najm, 2020).	14
Figure 3.1.2. Load versus maximum principle stress from FE and experimental results. (Choi and Najm, 2020)	14
Figure 3.1.3. Effect of base plate thickness (Choi and Najm, 2020).	15
Figure 3.1.4. Effect of number of stiffeners (Choi and Najm, 2020).	16
Table 2.2.1. Unstiffened socket connection test groups (Choi and Najm, 2020).	9
Table 2.3.1. Stiffened socket connection test groups (Choi and Najm, 2020).	12
Table 3.1.1. Effect of base plate thickness, number of stiffeners, galvanization, and peening on fatigue life, damage, and safety factor (Choi and Najm, 2020).....	16
Table 5.1. Fatigue Details (AASHTO, 2015).	18
Table 5.2. Fatigue Stress Concentration Factors, K_F (AASHTO, 2015).	20

1. INTRODUCTION

1.1. Highway Support Structures

Common highway support structures have a single support with a cantilevered arm supporting lights or signs, single support with a light or sign directly on top, or two or more supports with a truss supporting signs or overhead structures. Highway support structures are exposed to several wind phenomena that can produce cyclic loads. Cyclic loading is the application of repeated stresses to a location on a structural component. Vibrations caused by these cyclic forces can become substantial. Wind phenomena that have been found to produce cyclic loads, as described in the *Standard Specifications for Structural Supports for Highway Signs, Luminaires and Traffic Signals* published by the American Association of State Highway and Transportation Officials (AASHTO), are galloping, vortex shedding, natural wind gusts, and truck-induced gusts. Galloping is the sudden start of large amplitude wind vibrations that increase with increases in wind velocity. Vortex shedding occurs when wind blows across a structural member, creating vortices that are shed alternately from one side to the other, alternating low pressure zones, generating fluctuating forces acting at a right angle to the wind direction. These wind loadings can induce large amplitude vibrations and possibly cause fatigue damage in cantilevered support structures. Fatigue is the damage that may result in fracture after a sufficient number of stress fluctuations. Whenever a structure experiences fatigue damage, it may, in some cases, be repaired, or have to be replaced and replacement can be costly.

Often most fatigue damage is found at the connections in a support structure. Typical base plate connections attaching a support to a foundation are socket connections that have a round circular member inserted into a hole in a plate, plate with welded stiffeners, or a stiffened casting (shoe base) and fillet welds are placed between the pole and plate or casting on the outside and inside. A common shoe base plate (a), stiffened tube-to-transverse plate (b), and tube-to-transverse plate (c) connection are shown in Figure 1.1.1. The weld at the top of the base plate and tube is a fatigue strength design concern on support structures.



Figure 1.1.1. Shoe base plate (a), and stiffened (b) and unstiffened (c) tube-to-transverse base plate.

1.2. Fatigue and Fatigue Resistance

Accurate fatigue loads are generally not available when completing design calculations for highway support structures. Computation of stress fluctuations and the corresponding number of cycles for all wind-induced events is practically impossible. Real loads on structures are usually transient, variable, and complex. Sometimes it is not possible to simulate the field conditions because they are not known precisely (Agarwal et al., 1994). With this uncertainty,

the design of support structures for a finite fatigue life is unreliable. Therefore, an infinite life fatigue design approach is recommended (AASHTO, 2014). The infinite life fatigue approach ensures that a structure performs satisfactorily for its design life without significant fatigue damage.

An analysis was performed in the *AASHTO LRFD Bridge Design Specifications* for different structural joint details to obtain a curve defining the estimated mean life for a particular detail group. A detail group in this case consists of different types of connections, materials, and welds. A set of curves was developed for eight different detail stress categories ranging from stress category A to E', with A representing the highest fatigue resistance and E' representing the lowest fatigue resistance. The curves, specified in the *AASHTO LRFD Bridge Design Specifications*, are shown in Figure 1.2.1. Per the fifth edition of the *Standard Specifications for Structural Supports for Highway Signs, Luminaires and Traffic Signals*, hereafter referred to as the *Standard Specifications*, unstiffened tube-to-transverse plate connection details are classified as stress category E' and stiffened tube-to-transverse plate connection details are classified as stress category E.

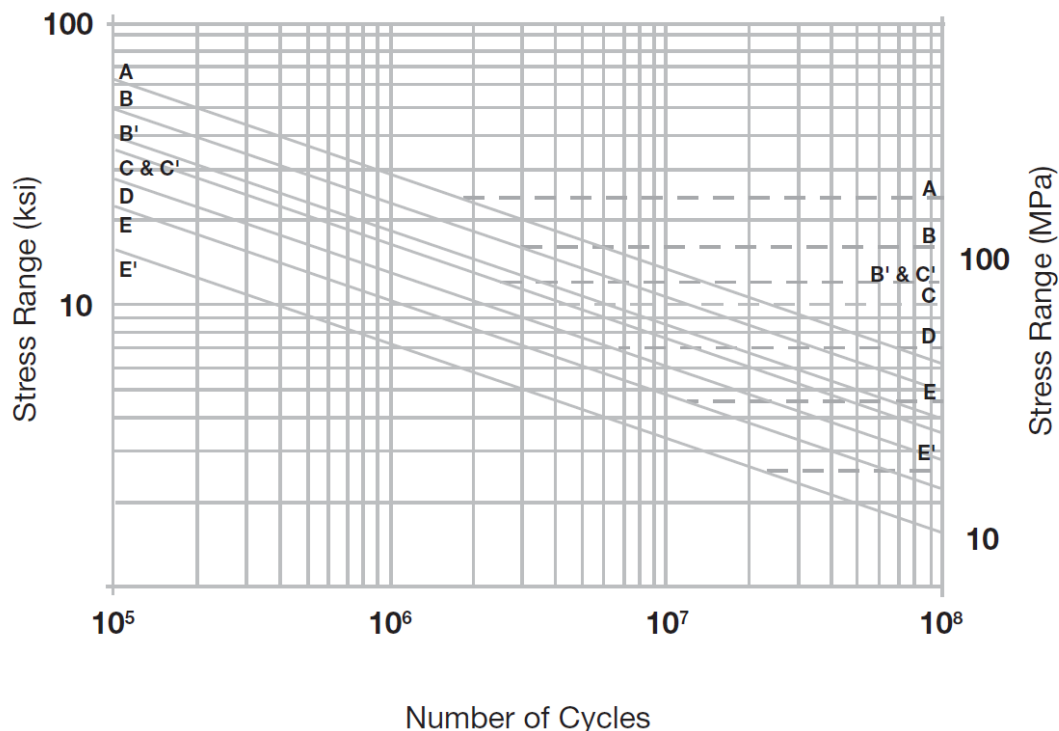


Figure 1.2.1. Stress Range vs. Number of Cycles (AASHTO LRFD, 2015).

Research (Roy et al., 2011) shows that the infinite life fatigue resistance of connection details in highway support structures do not always correspond to their respective finite life detail categories of the *AASHTO LRFD Bridge Design Specification* (AASHTO, 2014). The National Cooperative Highway Research Program (NCHRP) Project 10-70 tested the fatigue resistance of full-size steel support structure details to assist designers and the results are provided in Table 11.9.3.1-1 and 11.9.3.1-2 of the sixth edition of the *Standard Specifications*. The results further categorize detail groups for highway support structure connections based on type of connection, materials, and welds.

2. FATIGUE DESIGN AND RESEARCH

2.1. AASHTO Standard Specifications for Structural Supports

Common base plates are shown in Figure 1.1.1 for both steel and aluminum. The decision for the structure to be fabricated from steel or aluminum depends on the agency responsible for maintenance. The base plates are fabricated by inserting a thin walled tube into a hole in the base plate or stiffened casting, and a fillet-weld is used along the perimeter between the tube wall and the plate on the top outside, and bottom inside of the cut-out in the base plate. For base plates with welded stiffeners, fillet-welds are used along the perimeter between the tube wall, the plate, and the longitudinal attachments. The top weld is more structurally significant than the bottom since it resists both shear and tensile stresses.

The thin wall tube primarily carries load through in-plane stresses but near the supports, the tube-to-transverse-plate connection introduces out-of-plane flexural deformation, and therefore, causes out-of-plane bending stresses. Fatigue cracking at the weld toe begins from the high tensile residual stresses and weld geometry. The fillet-welded tube-to-transverse-plate connection was defined as stress category E' before the sixth edition of the *Standard Specifications*, but NCHRP Project 10-70 found fillet-welded tube-to-transverse-plate connections to have slightly higher constant amplitude fatigue thresholds (CAFTs) depending on the connection geometry. CAFTs are the stress amplitudes from loading that when below that level do not lead to failure, values above the threshold however, lead to crack initiation and crack growth to failure. The CAFT for infinite life design is determined from Table 11.9.3.1-1 (AASHTO, 2014). The stress induced by wind loads, $\gamma(\Delta f)_n$, should be below the CAFT,

$\phi(\Delta F)_{TH}$, for an infinite fatigue life resistance, $\phi(\Delta F)_n$, as shown in equation (1) (AASHTO, 2014):

$$\gamma(\Delta f)_n < \phi(\Delta F)_n = \phi(\Delta F)_{TH} \quad (1)$$

The value of $(\Delta F)_{TH}$ for aluminum structure details shall be determined by dividing the respective threshold values of steel by 2.6 (AASHTO, 2014). For infinite life design, the stress range must be below the CAFT for no crack to be anticipated. Typical weld details exhibit a CAFT at 10 to 20 million cycles which has been established for the fatigue design limit of highway support structures (Puckett et al., 2014).

The connection details of support structures in Table 11.9.3.1-1 (AASHTO, 2014) have certain limitations when determining the fatigue resistance because there are no considerations for the factors such as inherent defects in welding, galvanization, and mean and residual stress effects. Also, the CAFT is only applicable where geometries of the connection are within a certain range of dimension (Choi and Najm, 2020). The fatigue resistance is classified in Table 11.9.3.1-1 (AASHTO, 2014) by stress concentration factors K_F and K_I for finite and infinite life respectively. K_F for unstiffened and stiffened fillet-welded tube-to-transverse-plate connections are shown in Table 5.1 and Table 5.2 in Appendix A. K_I is calculated by equation (2) below:

$$K_I = [(1.76 + 1.83t_T) - 4.76 * 0.22^{K_F}] * K_F \quad (2)$$

The stress concentration factors are used to determine if Table 11.9.3.1-1 (AASHTO, 2014) can be used for connection fatigue design.

2.2. Unstiffened Socket Connection

Stress-cycle (S-N) curves are used in stress life analysis. The stress range has constant amplitude and measures the number of cycles to failure, A is the value of the intercept on the x-axis when the fatigue life curve is graphed in a log-log scale. According to the Miner's rule, the fatigue life curve is generally expressed by:

$$N * S_R^m = A \quad (3)$$

where m represents the slope of the linear line in a log-log scale (Choi and Najm, 2020). Fatigue tests compiled in the research by Choi and Najm, for tube-to-transvers plate connections were divided into eight groups for base plate thickness, peening, galvanizing, and the shape of the tube as shown in Table 2.2.1. In Figure 2.2.1, the chart compares the fatigue coefficient, A , also referred to as Finite Life Constant in the *Standard Specifications*, mean minus two standard deviations for the eight groups of test data. The mean minus two standard deviations is commonly used for design purposes used to establish a lower bound, and is associated with a 2.3% probability of failure (Fisher et al., 1998) (Schneider and Maddox, 2003). The AASTHO limits of the threshold, $(\Delta F)_{TH}$, and finite life constant, A , from Detail 5.4 in Table 11.9.3.1-1 (AASTHO, 2014), an unstiffened socket connection, are shown as Group 9 in Figure 2.2.1.

Table 2.2.1. Unstiffened socket connection test groups (Choi and Najm, 2020).

Group	plate thickness		peened	galvanized	tube shape		$A_{MEAN - 2\sigma}$	number of testing data
	$t \geq 50.8 \text{ mm}$	$t < 50.8 \text{ mm}$			round	multisided		
1	yes	no	no	no	yes	no	$1.04\text{E} + 08$	14
2	yes	no	no	yes	yes	no	$6.58\text{E} + 07$	30
3	yes	no	no	no	no	yes	$9.76\text{E} + 07$	8
4	no	yes	no	no	yes	no	$2.03\text{E} + 08$	17
5	no	yes	no	no	no	yes	$7.33\text{E} + 06$	9
6	no	yes	no	yes	yes	no	$2.65\text{E} + 07$	8
7	no	yes	yes	no	no	yes	$1.71\text{E} + 08$	8
8	no	yes	yes	no	yes	no	$2.25\text{E} + 08$	4

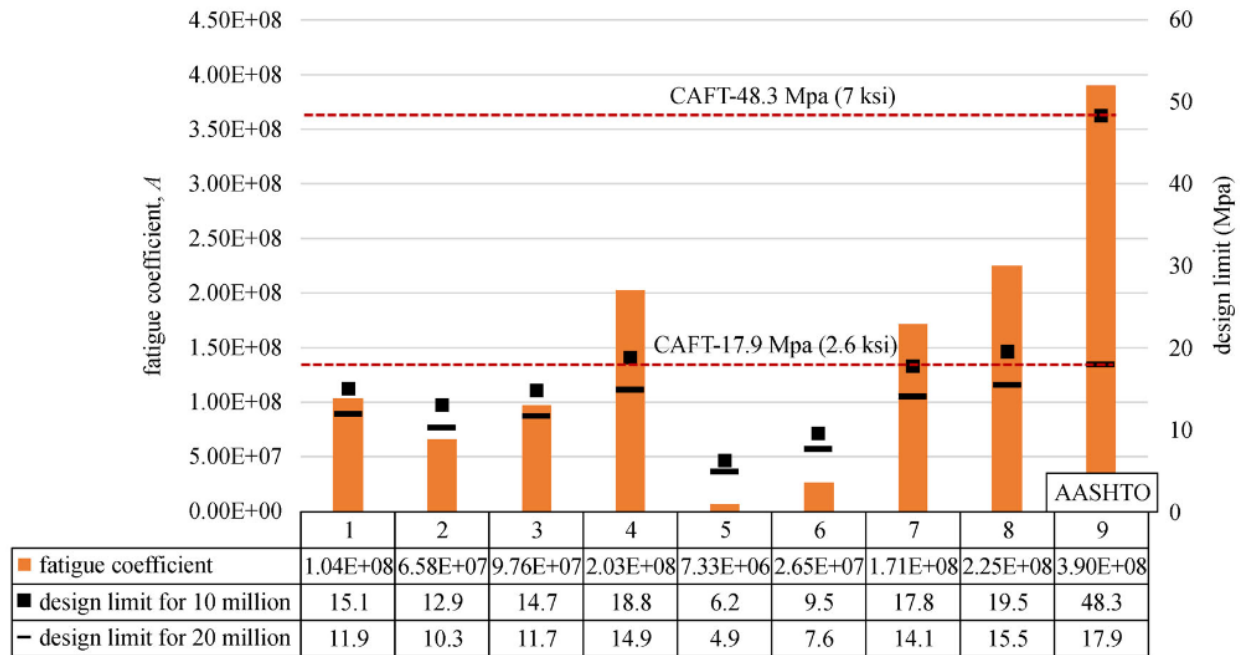


Figure 2.2.1. Unstiffened fatigue coefficients and design life (Choi and Najm, 2020).

Groups 1 and 2, and 4 and 6 show there is a reduction in fatigue design life with respect to galvanization. Also, there is a reduction in fatigue design life with respect to tube geometry. Groups 1 and 3, 4 and 5, and 7 and 8 show a reduction with multisided tubes, which is due to the stress concentrations that occur at the corners of the sides. It is observed that there is a reduction in fatigue design life for thin base plates between Groups 2 and 6, and 3 and 5. This aligns with previous research that has shown that the thickness of the base plate can increase the fatigue life (Stam et al., 2011). Group 4 however, has a larger fatigue design life than Group 1. Comparing Groups 5 and 7, and 4 and 8 shows an improvement in fatigue design life with respect to peening. Peening is a surface treatment for welding to help relieve tensile stresses that develop when the metal cools after welding. Group 5 shows the worst fatigue performance with a base plate thickness of 31.8 mm (1.25 inches), not peened, not galvanized, and multisided. Group 8 shows the best fatigue performance with a base plate thickness of 38.1 mm (1.5 inches), peened, not galvanized, and a round tube, although it should be noted only four tests were in this group.

When the fatigue design life for 10 and 20 million cycles in Group 9 are compared to each group, there are substantial discrepancies. Figure 2.2.1 displays that the AASHTO fatigue coefficient and CAFT of unstiffened socket connections are overly predicted when compared to

these compiled fatigue test results. Results from NCHRP Project 10-70 in Figure 2.2.2 for unstiffened socket connections show that the CAFT is estimated where run out begins for the connection, no crack propagates under stress. These results are where the limits for Group 9 in Figure 2.2.1 are from.

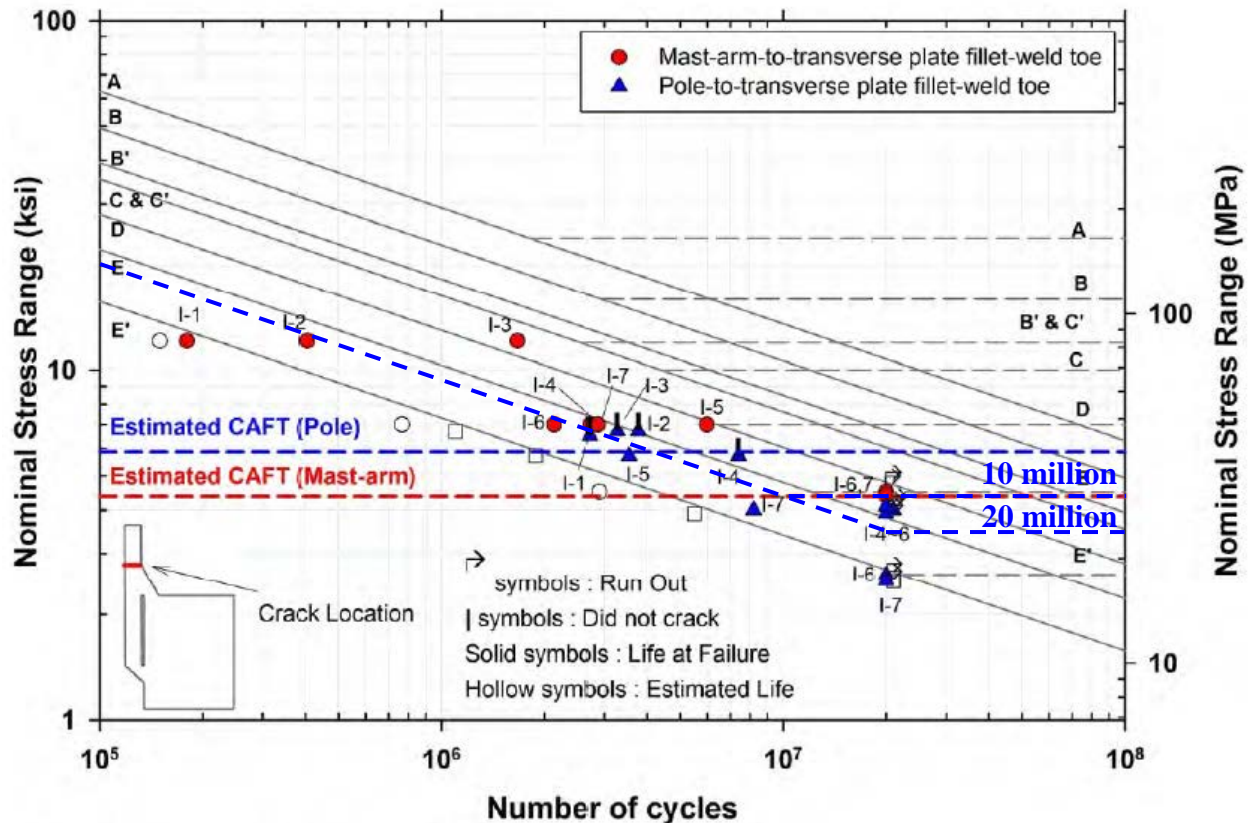


Figure 2.2.2. Fatigue test results for specimen Type I (Roy et al., 2011).

When the CAFT is compared to 10 and 20 million cycles for the fatigue design limit regression line, the CAFT appears to be lower at 31 MPa (4.5 ksi) and 25 MPa (3.6 ksi) respectively. If the fatigue limit with the mean minus two standard deviation regression line is calculated for the NCHRP data in Figure 2.2.2, the fatigue threshold and finite life constant would more reasonably be predicted for the compiled fatigue test results in Figure 2.2.1.

2.3. Stiffened Socket Connection

Similarly to the fatigue test results comparison of unstiffened tube-to-transverse plate connections by Choi and Najm, stiffened tube-to-transverse plate connections were compared.

The results were divided into three groups for failure location and number of stiffeners as shown in Table 2.3.1. Figure 2.3.1 compares the fatigue coefficient, A , mean minus two standard deviations for the three groups of test data with the AASTHO limits, Group 4, threshold, $(\Delta F)_{TH}$, and finite life constant, A , from Detail 6.2 in Table 11.9.3.1-1 (AASTHO, 2014), a stiffened socket connection.

Table 2.3.1. Stiffened socket connection test groups (Choi and Najm, 2020).

Group	failure location	number of stiffeners	$A_{MEAN-2\sigma}$	number of testing data
1	base	4-8	$9.46E+07$	15
2	stiffener	4	$2.90E+08$	16
3	stiffener	8	$4.74E+08$	12

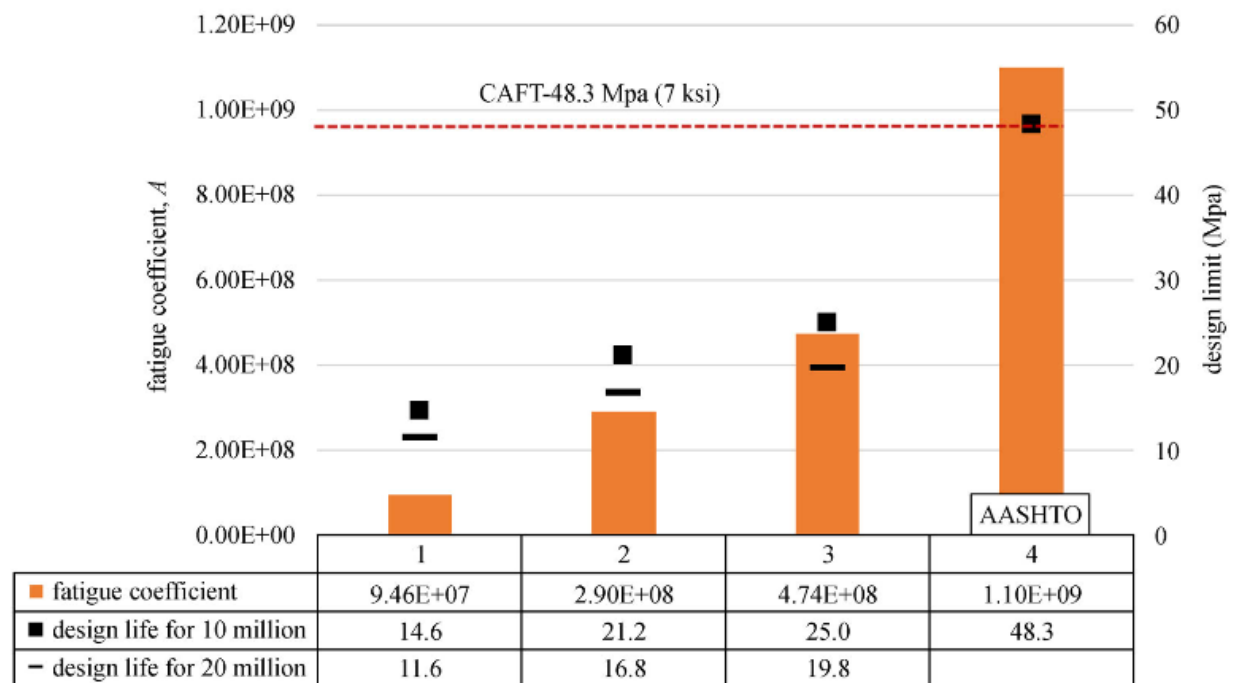


Figure 2.3.1. Stiffened fatigue coefficients and design life. (Choi and Najm, 2020).

The fatigue resistance of Group 1 is the lowest which has failure occurring at the base toe, indicating that local stresses were higher at the base toe than tip of the stiffeners. Failure of Groups 2 and 3 were located at the tip of the stiffeners. Group 3 had the best fatigue resistance with eight stiffeners. Again, when the fatigue design life for 10 and 20 million cycles in Group 4 are compared to each group, the AASHTO fatigue limit is overestimated. When the CAFT is

compared to 10 and 20 million cycles for the fatigue design limit regression line in Figure 2.3.2, the CAFT appears to be reasonably estimated. There is a need to verify these results with additional data and tests.

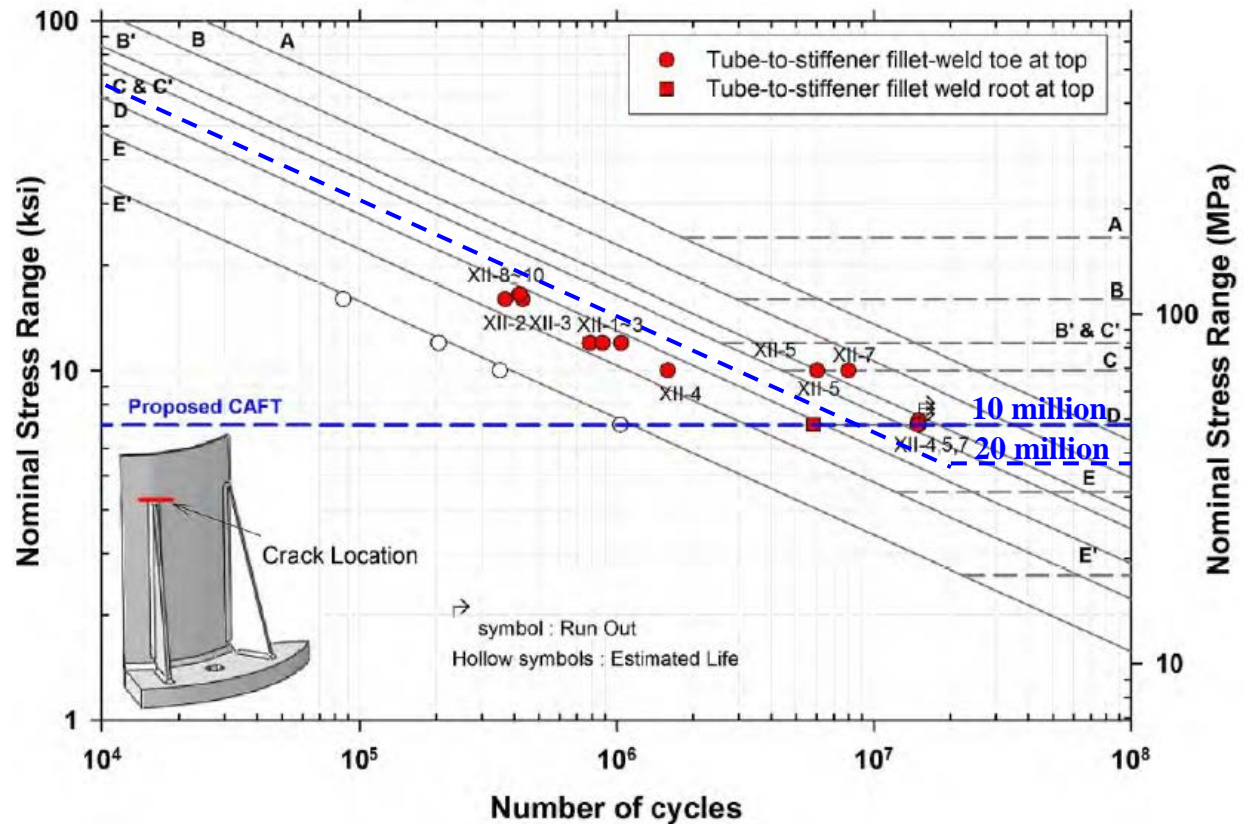


Figure 2.3.2. Fatigue test results for specimen Type XII at stiffener top (Roy et al., 2011).

3. FINITE ELEMENT ANALYSIS

3.1. Finite Element Model

A three-dimensional finite element (FE) model was developed by Choi and Najm in ANSYS Workbench 17 of a tube-to-transverse plate connection detail stiffened with eight welded stiffeners as shown in Figure 3.1.1. To validate the model, an identical stiffened tube-to-transverse plate connection detail was made of a tested specimen (Thompson W, 2012). Results of the model were compared to experimental results (Thompson W, 2012) in Figure 3.1.2 which displayed good correlation of FE results with experimental results.

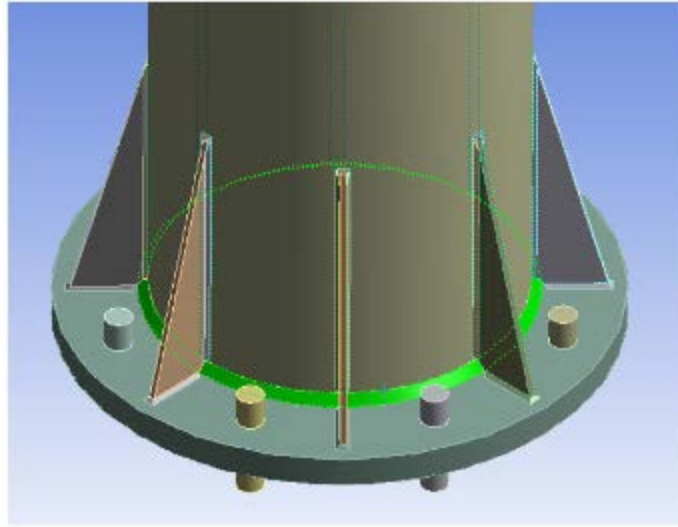


Figure 3.1.1. ANSYS stiffened socket connection (Choi and Najm, 2020).

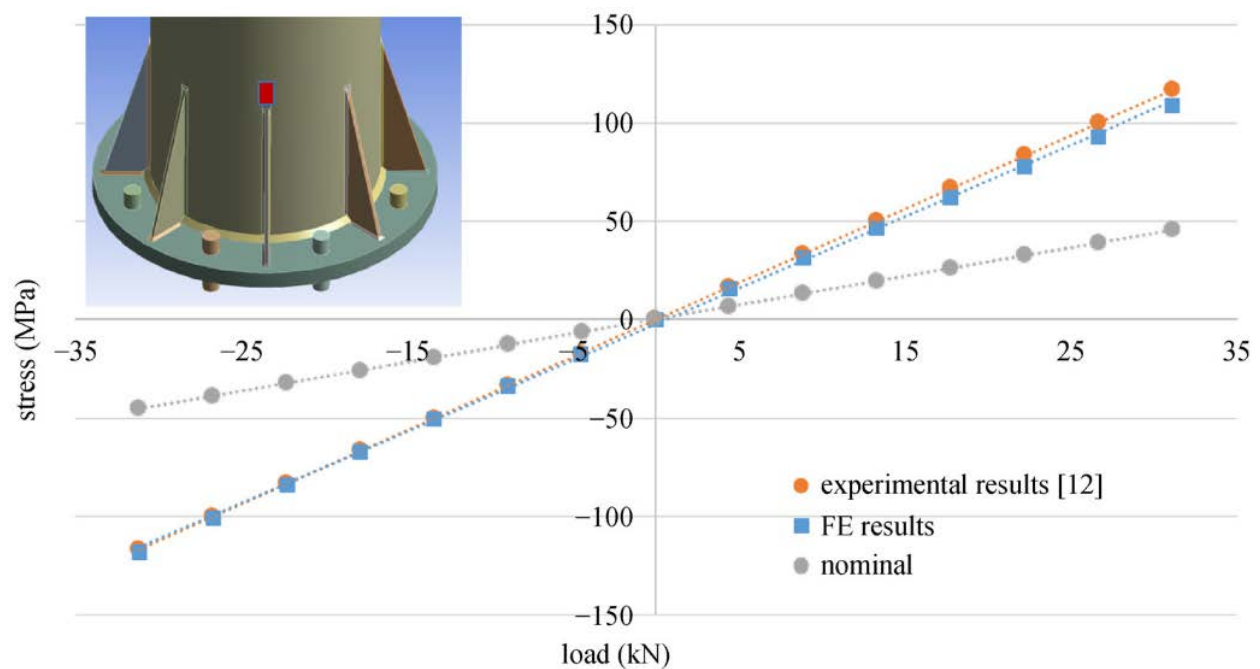


Figure 3.1.2. Load versus maximum principle stress from FE and experimental results. (Choi and Najm, 2020)

The FE model was evaluated by varying the base plate thickness, number of stiffeners, galvanization, and peening. Testing of multi-sided tubes was not considered. The stress range and number of cycles of the detail under constant amplitude stress life analysis and the fatigue

design life of Groups 1, 2, 4, 6, and 8 in Table 2.2.1 were input into the FE model. The model produced outputs of fatigue damage, factor of safety, and fatigue life. Fatigue life is the number of cycles to failure corresponding to the local principal stress while fatigue damage is the ratio of the design life to the available life.

The first model was evaluated at the fillet-welded connection with base plate thicknesses ranging from 38.1 mm (1.5 in) to 76.2 mm (3 in) and no stiffeners. Under constant applied force, the FE model shows a decrease in the local principal stress at the weld as the thickness of the base plate increases, shown in Figure 3.1.3, as expected.

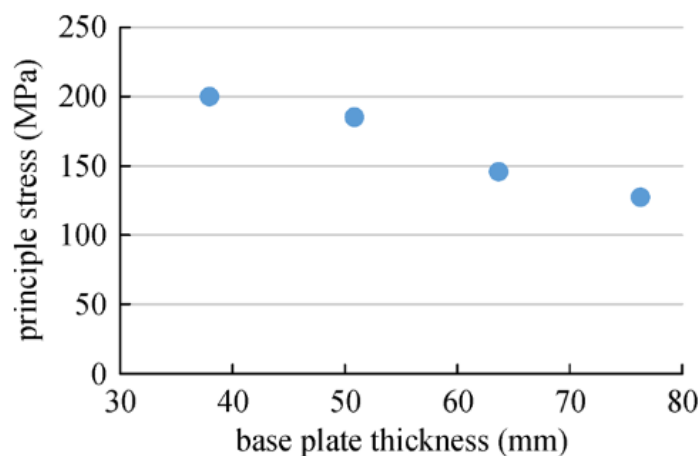


Figure 3.1.3. Effect of base plate thickness (Choi and Najm, 2020).

Next, effects of the number of stiffeners were tested. Maximum principal stress was located at the weld base toe for unstiffened socket connections and at the tip of the stiffeners for stiffened connections. The FE model was evaluated per the optimized stiffener configuration in the *Standard Specifications*. As shown in Figure 3.1.4, a connection with eight stiffeners has nearly half the maximum principal stress as an unstiffened connection. Also, it was observed that a connection with four stiffeners had similar local principal stress at the weld base toe and the tip of the stiffener (Choi and Najm, 2020).

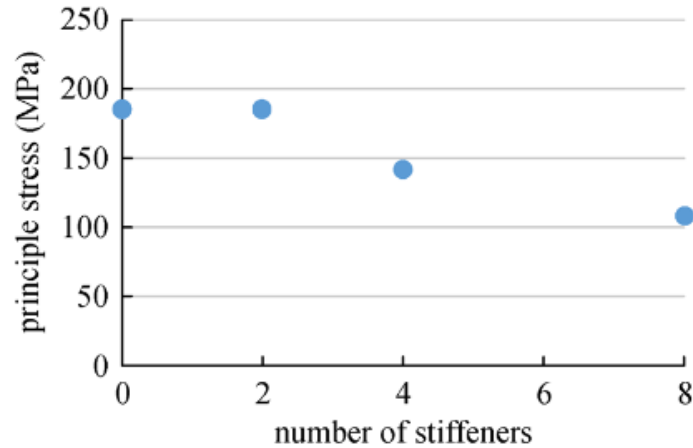


Figure 3.1.4. Effect of number of stiffeners (Choi and Najm, 2020).

Another model was created to evaluate the effects of galvanization on fatigue resistance. The fatigue curves of the test data of Groups 1 and 2 in Table 2.2.1 were used for the input. The FE analysis resulted in a fatigue life of $1.53\text{E}5$ cycles with a stress of 53.1 MPa without galvanization and a fatigue life of $9.70\text{E}4$ cycles with galvanization. These two models show there is a reduction in fatigue resistance due to galvanization. A similar result was found between Group 4 and 6. Results of the FE analysis are shown in Table 3.1.1.

Table 3.1.1. Effect of base plate thickness, number of stiffeners, galvanization, and peening on fatigue life, damage, and safety factor (Choi and Najm, 2020).

Group	base plate thickness (FE model)	stress range	life	damage	safety factor
1	50.8 mm	53.1 MPa	$1.53\text{E} + 05$	6.52 – 13.05	0.54 – 0.42
2	50.8 mm	53.1 MPa	$9.70\text{E} + 04$	10.31 – 20.62	0.46 – 0.36
4	38.1 mm	56.9 MPa	$2.53\text{E} + 05$	3.95 – 7.89	0.63 – 0.50
6	38.1 mm	56.9 MPa	$3.31\text{E} + 04$	30.2 – 60.5	0.32 – 0.25
8	38.1 mm	56.9 MPa	$2.81\text{E} + 05$	3.56 – 7.12	0.65 – 0.52

The purpose of galvanization is for corrosion resistance. Although there is an increase in fatigue resistance without galvanization, corrosion can more readily occur, thereby reducing the fatigue resistance. Other corrosion protection solutions could be researched in which the fatigue resistance is not affected by the process.

The last model was created to evaluate the effects of peening on fatigue resistance. The fatigue curves of the test data of Groups 4 and 8 in Table 2.2.1 were used for the input. The

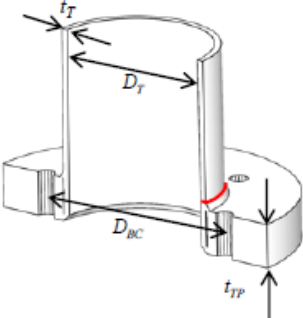
results of the FE analysis for Group 4 and 8 with a principle stress of 56.9 MPa are 2.53E5 and 2.81E5 cycles respectively. The results demonstrate that peening enhances the fatigue resistance.

4. SUMMARY

The fatigue resistance and fatigue life of fillet-welded stiffened and unstiffened socket connections were compared between the *Standard Specifications* Table 11.9.3.1-1 and lab research tests and finite element analysis. In addition to the difficulties to estimate loads on a highway support structure, there are many different geometries, materials, welds, and surface treatments for connections that can cause them to behave differently. Also, loads on real structures are variable, so for the constant amplitude fatigue thresholds to be conservative, they must be the near the max of the variable amplitude loading of real loads. For the design of stiffened and unstiffened socket connections, Table 11.9.3.1-1 (AASHTO, 2014) only takes dimensions of the connection geometry into account. Figures 2.2.2 and 2.3.2 show that the limits for Table 11.9.3.1-1 (AASHTO, 2014) may need adjusted. As was shown in Figure 2.2.1 and Figure 2.3.1, other factors can greatly change the fatigue resistance of connection details. Galvanization was found to decrease the fatigue resistance and peening was found to increase the fatigue resistance. Furthermore, the data compiled by Choi and Najm appears to show that the AASHTO limits overestimate the fatigue resistance of the tube-to-transverse-plate connection details. There is still a need for additional fatigue testing to verify the results from this completed study and the effects of surface treatments.

5. APPENDIX A

Table 5.1. Fatigue Details (AASHTO, 2015).

Description	Identification of Parameters	Tube Configuration	Detail Parameters	Finite Life Constant, $A \times 10^8$ (MPa ³ (ksi ³))	Threshold, ΔF_{TH} (MPa (ksi))
Fillet-welded tube-to-transverse-plate connections		Round	$t_T = 4.5 \text{ mm (0.179 in.)}$ $D_T = 254 \text{ mm (10 in.)}$ $t_{TP} = 51 \text{ mm (2 in.)}$ $D_{BC} = 592 \text{ mm (23.3 in.)}$ $N_B = 4$	1330 (3.9) ($K_F = 2.8$)	31 (4.5) ($K_I = 5.6$)
		Round	$t_T = 6.1 \text{ mm (0.239 in.)}$ $D_T = 330 \text{ mm (13 in.)}$ $t_{TP} = 51 \text{ mm (2 in.)}$ $D_{BC} = 508 \text{ mm (20 in.)}$ $N_B = 4$	1330 (3.9) ($K_F = 2.9$)	31 (4.5) ($K_I = 6.2$)
		Multisided	$t_T = 4.8 \text{ mm } (^{3/16} \text{ in.})$ $D_T = 254 \text{ mm (10 in.)}$ $t_{TP} = 51 \text{ mm (2 in.)}$ $D_{BC} = 592 \text{ mm (23.3 in.)}$ $N_B = 4$ $N_5 = 8$ $r_b = 13 \text{ mm (0.5 in.)}$	1330 (3.9) ($K_F = 3.2$)	18 (2.6) ($K_I = 6.6$)
		Multisided	$t_T = 6.4 \text{ mm } (^{1/4} \text{ in.})$ $D_T = 330 \text{ mm (13 in.)}$ $t_{TP} = 51 \text{ mm (2 in.)}$ $D_{BC} = 508 \text{ mm (20 in.)}$ $N_B = 4$ $N_5 = 8$ $r_b = 13 \text{ mm (0.5 in.)}$	($K_F = 3.5$)	18 (2.6) ($K_I = 7.6$)
		Multisided	$t_T = 7.9 \text{ mm } (^{5/16} \text{ in.})$ $D_T = 610 \text{ mm (24 in.)}$ $t_{TP} = 76 \text{ mm (3 in.)}$ $D_{BC} = 762 \text{ mm (30 in.)}$ $N_B = 16$ $N_5 = 16$ $r_b = 102 \text{ mm (4 in.)}$	1330 (3.9) ($K_F = 2.9$)	31 (4.5) ($K_I = 6.5$)

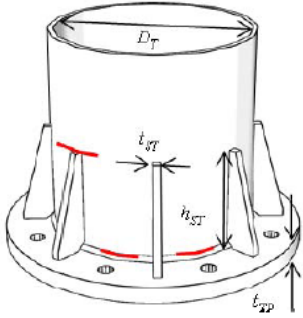
Description	Identification of Parameters	Tube Configuration	Detail Parameters	Finite Life Constant, $A \times 10^8$ (MPa ³ (ksi ³))	Threshold, ΔF_{TH} (MPa (ksi))
Tube-to-transverse-plate connections stiffened by longitudinal attachments with partial- or full-penetration groove welds, or fillet welds in which the tube is subjected to longitudinal loading and the welds are wrapped around the attachment termination.		Multisided	$t_T = 7.9 \text{ mm } (\frac{5}{16} \text{ in.})$ $D_T = 610 \text{ mm (24 in.)}$ $t_{TP} = 51 \text{ mm (2 in.)}$ $D_{BC} = 762 \text{ mm (30 in.)}$ $N_B = 8$ $N_S = 16$ $r_b = 102 \text{ mm (4 in.)}$ $N_{ST} = 8$ $h_{ST} = 457 \text{ mm (18 in.)}$ $t_{ST} = 9.5 \text{ mm } (\frac{3}{8} \text{ in.})$	Cracking at top of stiffener 3750 (11.0) ($K_F = 2.4$)	48 (7.0) ($K_T = 5.3$)
				Cracking at end plate fillet-weld toe on tube wall 1330 (3.9) ($K_F = 1.9$)	31 (7.0) ($K_T = 4.0$)

Table 5.2. Fatigue Stress Concentration Factors, K_F (AASHTO, 2015).

Section Type	Detail	Location	Fatigue Stress Concentration Factor for Finite Life, K_F	
Round	Fillet-welded tube-to-transverse-plate connections	Fillet-weld toe on tube wall	<u>SI Units</u> $K_F = 2.2 + 25(7t_T + 24) \times (D_T^{1.2} - 500) \times (C_{BC}^{0.03} - 1) \times t_{TP}^{-2.5}$ Valid for: $5 \text{ mm} \leq t_T \leq 13 \text{ mm}$ $203 \text{ mm} \leq D_T \leq 1270 \text{ mm}$ $51 \text{ mm} \leq t_{TP} \leq 102 \text{ mm}$ $1.25 \leq C_{BC} \leq 2.5$ <u>U.S. Customary Units</u> $K_F = 2.2 + 4.6(15t_T + 2) \times (D_T^{1.2} - 10) \times (C_{BC}^{0.03} - 1) \times t_{TP}^{-2.5}$ Valid for: $0.179 \text{ in.} \leq t_T \leq 0.5 \text{ in.}$ $8 \text{ in.} \leq D_T \leq 50 \text{ in.}$ $2 \text{ in.} \leq t_{TP} \leq 4 \text{ in.}$ $1.25 \leq C_{BC} \leq 2.5$	(11.9.3.1-2)
	Groove-welded tube-to-transverse-plate connections	Groove-weld toe on tube wall	<u>SI Units</u> $K_F = 1.35 + 33(7t_T + 12) \times (D_T - 130) \times \left(\frac{C_{BC}^{0.02} - 1}{4C_{OP}^{-0.7} - 3} \right) \times t_{TP}^{-2}$ Valid for: $5 \text{ mm} \leq t_T \leq 16 \text{ mm}$ $203 \text{ mm} \leq D_T \leq 1270 \text{ mm}$ $51 \text{ mm} \leq t_{TP} \leq 102 \text{ mm}$ $1.25 \leq C_{BC} \leq 2.5; 0.3 \leq C_{OP} \leq 0.9$ <u>U.S. Customary Units</u> $K_F = 1.35 + 16(15t_T + 1) \times (D_T - 5) \times \left(\frac{C_{BC}^{0.02} - 1}{4C_{OP}^{-0.7} - 3} \right) \times t_{TP}^{-2}$ Valid for: $0.179 \text{ in.} \leq t_T \leq 0.625 \text{ in.}$ $8 \text{ in.} \leq D_T \leq 50 \text{ in.}$ $2 \text{ in.} \leq t_{TP} \leq 4 \text{ in.}$ $1.25 \leq C_{BC} \leq 2.5$ $0.3 \leq C_{OP} \leq 0.9$	(11.9.3.1-3)

Section Type	Detail	Location	Fatigue Stress Concentration Factor for Finite Life, K_F	
Round	Fillet-welded tube-to-transverse-plate connections stiffened by longitudinal attachments	Weld toe on tube wall at the end of attachment	<u>SI Units</u> $K_F = \frac{1}{1000} \left(79 \frac{t_{ST}^{0.4}}{t_T^{0.7}} + 9 \right) \times \left(\frac{D_T^{0.8}}{N_{ST}^{1.2}} + 30 \right)$ Valid for: $6 \text{ mm} \leq t_{ST} \leq 22 \text{ mm}$ $6 \leq N_{ST} \leq 12$ $8 \text{ mm} \leq t_T \leq 16 \text{ mm}$ $610 \text{ mm} \leq D_T \leq 1270 \text{ mm}$ <u>U.S. Customary Units</u> $K_F = \left(\frac{t_{ST}^{0.4}}{t_T^{0.7}} + 0.3 \right) \times \left(0.4 \frac{D_T^{0.8}}{N_{ST}^{1.2}} + 0.9 \right)$ Valid for: $0.25 \text{ in.} \leq t_{ST} \leq 0.875 \text{ in.}$ $6 \leq N_{ST} \leq 12$ $0.3125 \text{ in.} \leq t_T \leq 0.625 \text{ in.}$ $24 \text{ in.} \leq D_T \leq 50 \text{ in.}$	(11.9.3.1-4)
	Fillet-welded tube-to-transverse-plate connections stiffened by longitudinal attachments	Fillet-weld toe on tube wall	<u>SI Units</u> $K_F = \left[\left(80 \frac{D_T^{0.15}}{N_{ST}^{1.5}} + 1 \right) \times \left(\frac{3.3}{h_{ST} + 178} \right) \times \left(\frac{33}{t_{ST}^{0.5}} - 1 \right) \right]$ $\times K_F \text{ as per Eq. 11.9.3.1-1}$ Valid for: $305 \text{ mm} \leq h_{ST} \leq 1067 \text{ mm}$ $6 \text{ mm} \leq t_{ST} \leq 22 \text{ mm}; 6 \leq N_{ST} \leq 12$ $610 \text{ mm} \leq D_T \leq 1270 \text{ mm}$ <u>U.S. Customary Units</u> $K_F = \left[\left(130 \frac{D_T^{0.15}}{N_{ST}^{1.5}} + 1 \right) \times \left(\frac{0.13}{h_{ST} + 7} \right) \times \left(\frac{6.5}{t_{ST}^{0.5}} - 1 \right) \right]$ $\times K_F \text{ as per Eq. 11.9.3.1-1}$ Valid for: $12 \text{ in.} \leq h_{ST} \leq 42 \text{ in.}$ $0.25 \text{ in.} \leq t_{ST} \leq 0.875 \text{ in.}$ $6 \leq N_{ST} \leq 12$ $24 \text{ in.} \leq D_T \leq 50 \text{ in.}$	(11.9.3.1-5)

Section Type	Detail	Location	Fatigue Stress Concentration Factor for Finite Life, K_F	
Multisided	As above	As above	Multiply respective K_F above (except for Eq. 11.9.3.1-4) by: <u>SI Units</u> $\left[1 + \frac{1}{25} (D_T - r_b) \times N_S^{-2} \right]$ Valid for: $203 \text{ mm} \leq D_T \leq 1270 \text{ mm}$ $25 \text{ mm} \leq r_b \leq 102 \text{ mm}$ $8 \leq N_S \leq 16$ <u>U.S. Customary Units</u> $\left[1 + (D_T - r_b) \times N_S^{-2} \right]$ Valid for: $8 \text{ in.} \leq D_T \leq 50 \text{ in.}$ $1 \text{ in.} \leq r_b \leq 4 \text{ in.}$ $8 \leq N_S \leq 16$	(11.9.3.1-6)

6. REFERENCES

AASHTO. *LRFD Bridge Design Specifications*. American Association of State Highway and Transportation Officials, Washington, DC, 2015.

AASHTO. *Standard Specifications for Structural Supports for Highway Signs, Luminaires, and Traffic Signals*. 6th ed, 2015 Interim Revisions. American Association of State Highway and Transportation Officials, Washington, DC, 2014.

Agarwal A, Birkemoe P, Hoel A, Sweeney R, Thompson J, Topper T. *Issues in Structural Fatigue Design and Evaluation*. 21(6):903-912. Canadian Journal of Civil Engineering, 1994.

ASM International. 'Fatigue'. *Elements of Metallurgy and Engineering Alloys*. ASM International, 2008.

Choi H, Najm H. 2020. *Investigation of fatigue resistance of fillet-welded tube connection details for sign support structures*. 14(1), 199-214. Frontiers of Structural & Civil Engineering, 2020.

Concord American. 80 Spun Collars. Concord American Flagpole, 2018.

(<https://www.concordamericanflagpole.com/components/collars/>)

Fisher J, Kulak G, Smith I. *A fatigue primer for structural engineers*. Chicago, IL: National Steel Bridge Alliance, American Institute of Steel Construction, 1998.

Puckett J A, Garlich M G, Nowak A A, Barker M. *Development and Calibration of AASHTO LRFD Specifications for Structural Supports for Highway Signs, Luminaires, and Traffic Signals*. Report No. Project 10-80, 2014.

Roy S, Park Y C, Sause R, Fisher J W. *Fatigue performance of stiffened pole-to-base plate socket connections in high-mast structures*. 138(10):1203–1213. Journal of Structural Engineering, 2012. (<https://ascelibrary.org/cms/asset/4d2b8be9-7421-4d85-a197-9e23431f9476/figure4.jpg>)

Roy, S., Y. C. Park, R. Sause, J. W. Fisher, and E. K. Kaufmann. *Cost-Effective Connection Details for Highway Sign, Luminaire and Traffic Signal Structures*. NCHRP Web Only Document 176, Final Report for NCHRP Project 10-70. Transportation Research Board, National Research Council, Washington, DC, 2011.

Schneider C R A, Maddox S. *Best Practice Guide on Statistical Analysis of Fatigue Data*. Cambridge: International Institute of Welding, 2003.

Stam A, Richman N, Pool C, Rios C, Anderson T, Frank K. *Fatigue Life of Steel Base Plate to Pole Connections for Traffic Structures*. Report No. FHWA/TX-11/9-1526-1, 9-1526-1, 2011.

Thompson W. *Evaluation of high-level lighting poles subjected to fatigue loading*. Thesis for the Master's Degree. Bethlehem: Lehigh University, 2012.